Atomic Force Microscopy Characterization of Ultrathin Polystyrene Films Formed by Admicellar Polymerization on Silica Disks

Chun Hwa See, John O'Haver

Department of Chemical Engineering, University of Mississippi, Oxford, Mississippi 38677

Received 15 February 2002; accepted 18 September 2002

ABSTRACT: Atomic force microscopy was used to study the characteristics of polymer films formed via admicellar polymerization (the polymerization of monomers solubilized in adsorbed surfactant aggregates). The investigated system included cetyltrimethylammonium bromide (C_{16}TAB) as a cationic surfactant, styrene, 2,2′-azobisisobutyrilnitrile as an initiator, and polished silica disk substrates. Our goal was to examine changes in the properties and morphology of the formed polymer films due to changes in the surfactant and monomer feed levels. Normal tapping and phase-contrast modes in air were used to image the nanoscopic and microscopic morphologies of the polystyrene-modified silica. The root-mean-square roughness of the surface before and after modification was statistically analyzed and compared. The images were captured with loading-force setpoint ratios of 0.2–0.9, and this allowed us to examine the stability of the polystyrene films. In the first series, for which the feed ratio of C_{16}TAB to styrene was kept constant and the total feed concentration was varied, a uniform layer of a polystyrene film was observed along with some nanometer-size aggregates at high feed concentrations of both C_{16}TAB and styrene. These droplets eventually agglomerated with the film beneath and formed larger macrodroplets in a ring arrangement. At lower concentrations, droplets and holes were observed that eventually agglomerated to form a bicontinuous thin film. In the second experimental series, the concentration of C_{16}TAB was kept constant, and the feed ratio of C_{16}TAB to styrene was varied. A smooth thin film was observed at high concentrations of styrene. This film could be deformed and/or removed to expose the silica surface beneath. At lower styrene loadings, the polystyrene film became unstable and formed dropletlike aggregates, possibly because of either the uneven adsolubilization of the styrene monomer within the admicelle or the dewetting effect during washing and drying. The structure of the polystyrene film formed on a smooth silica disk was very dependent on the amount of the surfactant fed to the system; this contrasted with the results on precipitated silica. © 2003 Wiley Periodicals, Inc. J Appl Polym Sci 89: 36–46, 2003

Key words: composites; interfaces; nanoheterogeneity; polystyrene; thin films

INTRODUCTION

Admicellar polymerization, or the polymerization of monomers solubilized in adsorbed surfactant aggregates, was first developed in the 1980s[1–3] as a means of modifying the surfaces of various substrates. The process has been characterized as occurring in four steps: (1) surfactant adsorption/admicelle formation, (2) adsolubilization of monomer(s), (3) polymerization, and (4) surfactant removal. The process has been used to modify the surface properties of various kinds of substrates, such as glass fibers,[1] alumina,[2–4] amorphous silica,[5–8] titanium oxide,[9] glass cloth,[10] and nickel.[11] Polymer thin films have been studied with various methods, including scanning electron microscopy,[2,3] ellipsometry,[9,10] Fourier transform infrared spectroscopy,[3,8] evaluation of the wearing properties of composites,[3] scanning tunneling microscopy,[11] and contact-mode atomic force microscopy (AFM).[5,11] These studies have not provided insights into any changes that may occur in the characteristics and morphology of polymer films because of changes in the admicellar polymerization process, specifically changes in the concentrations of the surfactant and monomer(s). Acquiring a better understanding of the distribution and characteristics of the polymer films formed by this process could be important to the various current and potential applications of the process.

Correspondence to: J. O'Haver (johaver@olemiss.edu).

Contract grant sponsor: National Science Foundation; contract grant number: 9724187.

Contract grant sponsors: University of Mississippi Loyalty Foundation; University of Mississippi Associates and Partners Program.

Journal of Applied Polymer Science, Vol. 89, 36–46 (2003)

EXPERIMENTAL

Materials

The surfactant was 99% pure cetyltrimethylammonium bromide (C_{16}TAB) from Sigma Chemical (St. Louis, MO). Styrene, 99% pure, was also purchased from Sigma Chemical. 2,2′-Azobisisobutyronitrile

(AIBN; 99% pure) was obtained from Aldrich (Milwaukee, WI). Polished silica disks were obtained from Heraeus-Amersil, Inc. (Duluth, GA). The disks were 0.413 in. in diameter and 0.039 in. thick. All the materials were used as received. Deionized water was obtained with a Barnstead E-pure water system (Dubuque, IA) with a resistivity of 18.3 MΩ cm.

AFM

An atomic force microscope was obtained from Digital Instruments, Inc. (Santa Barbara, CA). Topographic and phase images were captured simultaneously with tapping-mode AFM. Imaging was performed with 125-μm silicon tips obtained from Digital Instruments, Inc. Set-point ratios (ratio of the engage oscillation amplitude to the free air oscillation amplitude) of 0.2–0.9 were used for the imaging of all topographic and phase images unless otherwise stated. The thickness of the polystyrene films was analyzed with cross-section analysis software provided in Nanoscope IIIa (version 4.23r23; Digital Instruments). Although the root-mean-square roughness was measured on at least 10 different sites and also with at least five different scan sizes ranging from 250 nm to 50 μm, the root-mean-square roughness listed was measured obtained by random measuring within an area of 250 nm $\times$ 250 nm (unless otherwise stated). Therefore, although root-mean-square roughness (R_g) is not a linear function of the scan size, maintaining a constant scan size eliminates this problem. All the samples were imaged at ambient temperatures in air with a relative humidity of 30–50%. All physical features discussed in the following sections were characteristic of the samples, that is, widely and uniformly found, not anomalies or singularities. The same tip was used to measure the roughness of different samples and was cleaned with methanol and water between runs so that contamination artifacts would be eliminated. The samples were stored at ambient temperature (22–24°C) in covered containers.

Surface-modification procedure

The critical micelle concentration value of C_{16}TAB, approximately 850 μM, was obtained from the adsorption isotherm data of C_{16}TAB on Hi Sil 233.[12] To avoid micelle formation in the solution, which would lead to emulsion polymerization, we kept the equilibrium concentration of C_{16}TAB at approximately 750 μM. The feed concentration of the adsolubilized styrene monomer was based on the amount of adsorbed C_{16}TAB. The silica disk was atomically smooth and had a root-mean-square roughness of 0.7 nm. For this reason, we assumed the surface area of the silica disk was equal to $2\pi r(r + t)$, where t is the thickness of the disk. The adsorbed C_{16}TAB was assumed to form complete bilayers on the surface of the silica disk with an area per head group of 91 A^2 at air–water interfaces.[13]

Silica has a point of zero charge (pzc) between pH 2 and 3.[14] At pHs below the pzc, the surface of silica will be protonated and have a net positive charge; at pHs above the pzc, the silica surface will be negatively charged. Therefore, pHs above the pzc provided a surface suitable for the adsorption of cationic C_{16}TAB. In this experiment, the adsorption and adsolubilization studies were carried out at $7 < pH < 8$ by adjustments to the feed solutions with a dilute sodium hydroxide solution. The mixtures were stirred in a cold water bath for 12 h before being placed with the silica disk in a 20-mL vial. The samples were allowed to sit refrigerated for at least 4 days to equilibrate. After that, the polymerization was carried out by the samples being heated to 70°C for 24 h. After the polymerization, the samples were washed with slow, continuous flushing with 5 gallons of deionized water. The disks were then dried overnight at 40°C. The modified disks were kept in clean vials inside a desiccator until they were examined. The silica disks were mounted onto a 12-mm metal plate with double-sided tape for scanning. The experimental plan is shown in Table I.

RESULTS

Unmodified silica

A topographic image of the unmodified, polished silica disk is shown in Figure 1. The surface was smooth, with only minor irregularities. The root-mean-square roughness was measured to be 0.7 $\pm$ 0.07 nm. No significant changes in the phase and topographic images of the unmodified silica disks were observed as the set-point ratio was varied from 0.2 to 0.9 and the scanning rate was varied from 0.2 to 2.4 Hz. There was no appreciable phase shift of the unmodified silica disk, as expected for a homogeneous surface.

Constant ratio of the initial C_{16}TAB concentration to the styrene concentration (series DI)

When the silica surface was modified by a feed of 750 μM C_{16}TAB and 863 μM styrene (sample DI-1), we observed several polystyrene droplets on a thin and uniform polystyrene film (Fig. 2). The root-mean-square roughness for this sample was 0.53 $\pm$ 0.1 nm, lower than that of the unmodified silica surface. The reduction in the roughness can be explained by the formation of a smooth polystyrene film on top of the silica surface, despite the additional roughness caused by the polymer droplets, which had an average diameter of 19.2 $\pm$ 3.4 nm and an average height of 1 $\pm$ 0.23 nm. The polystyrene film was quite stable, with no deformation observed even under a higher tapping force (set-point ratio of 0.2). Some of the polymer

TABLE I
Experimental Plan Examining Different Feed Concentrations with the Surfactant/Monomer ratio Kept Constant and Different Monomer Feed Concentrations with the Feed Surfactant Concentration Kept Constant

Silica disk sample	C_1TAB (μM)	AIBN (μM)	Styrene (μM)	Surfactant feed concentration/ feed concentration of sample I-D1
DI-1	750	12.5	863	1
DI-2	500	12.5	595	1/1.5
DI-3	250	12.5	297	1/3
DI-4	50	12.5	58	1/15
			Nanomolar	Ratio of adsorbed C_{16}TAB to adsolubilized styrene monomer
DII-1	750	12.5	10.83	2.0:1
DII-2	750	12.5	8.67	2.5:1
DII-3	750	12.5	6.50	3.3:1
DII-4	750	12.5	2.17	10.0:1

aggregates on the surface were as large as 140 nm in diameter and 2.1 nm in height. The sample was imaged over a period of several weeks and showed no measurable change during this period. However, when the same sample was imaged more than a year later, the polystyrene film had agglomerated, forming aggregates with diameters ranging from 156 to 430 nm and thicknesses ranging from 13 to 27 nm. Some of these structures were arranged in straight lines with average diameters of 156–430 nm and heights of 13–27 nm (Fig. 3). Ringlike structures with two different average diameters, one approximately 300 nm and the other approximately 1 μm (Fig. 4), were also observed. The data indicate that at least some of these droplets were hollow hills; that is, that they could deform or collapse with additional pressure. Therefore, the use of the term *droplet* is intended to convey their shape, but not necessarily their structure.

Sample DI-2 had a feed concentration of 500 μM C_{16}TAB and 595 μM styrene (66% of that in DI-1). The polystyrene film that formed showed the presence of droplets and holes [Fig. 5(a)]. These droplets had diameters averaging 38.4 $\pm$ 7.2 nm and average heights of 3 $\pm$ 1 nm, approximately two times the size of the droplets observed in sample DI-1. The root-mean-square roughness of sample DI-2 was also higher (1.08 $\pm$ 0.25 nm). During imaging under a higher tapping force, some of these droplets collapsed [Fig. 5(b)]. The observed holes had an average depth of 4 nm. When sample DI-2 was reimaged a year later, areas of uniform polystyrene film coexisted with irregular patches of disturbed film (when observed on the micrometer scale; see Fig. 6). Portions of the film appeared to be folding to form ridges and valleys, indications that they were not well attached to the surface (see arrow

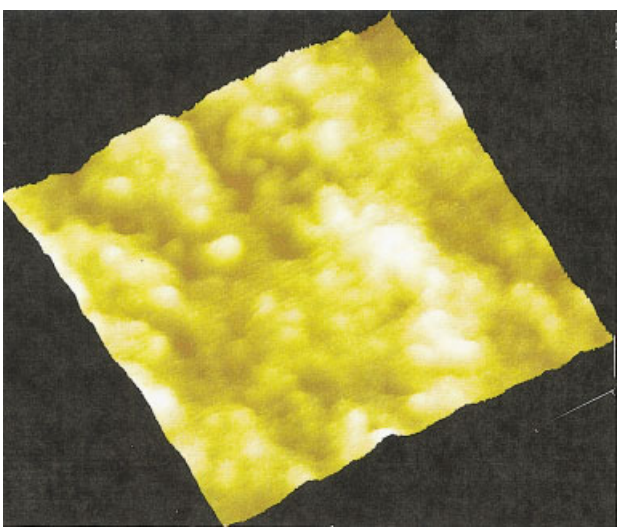

Figure 1 Topographic image of an unmodified silica disk. The imaging area is 400 nm $\times$ 400 nm, with a z range of 10 nm.

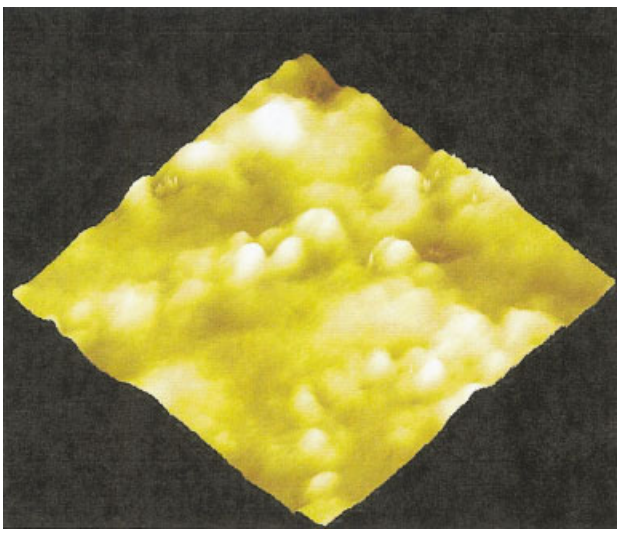

Figure 2 Topographic image of polymer-modified silica (sample DI-1, modified by a feed of 750 μM C_{16}TAB and 893 μM styrene). The imaging area is 400 nm $\times$ 400 nm, with a z range of 10 nm.

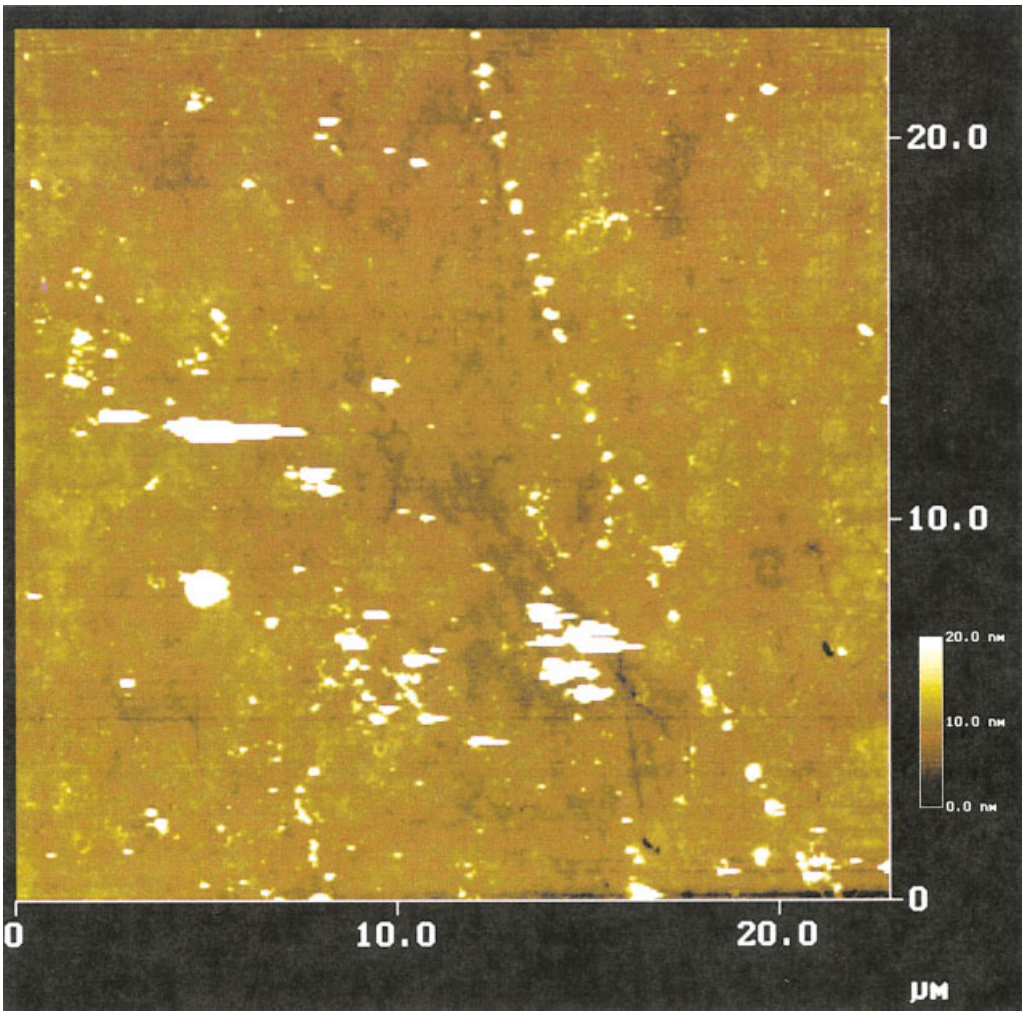

Figure 3 Microscopic topographic image of sample DI-1 scanned after a year. Aggregates of polystyrene can be seen in straight-line formations, with diameters ranging from 156 to 430 nm and heights ranging from 13 to 27 nm. Larger aggregates deformed by the tip can also be observed scattered on the surface. The imaging area is 22.9 μm $\times$ 22.9 μm, with a z range of 20 nm.

A in Fig. 6 and the three-dimensional image in Fig. 7). Some of the polystyrene nucleated to form droplets (shown as arrow B in Figs. 6 and 7). Phase imaging was able to distinguish the composition of the surface at a set-point ratio of 0.9. The areas of brighter contrast in Figure 6 indicate the polystyrene film, and those of darker contrast represent the exposed silica surface. When the set-point ratio was decreased to 0.7 (increasing the force), we expected the soft polymer areas to appear darker by contrast. However, the polystyrene film was deformed or removed with imaging at this set-point ratio. The thickness of the uniform polystyrene films were 5–10 nm, whereas the nucleated droplets ranged in size from 80 to 150 nm.

Sample DI-4 had feed concentrations of C_{16}TAB and styrene of 50 and 58 μM, respectively (6.5% of that in sample DI-1). Immediate imaging showed a significant number of polystyrene droplets on the surface (Fig. 8). The average diameter of the observed droplets was 24.5 $\pm$ 3.4 nm, with an average height of 1.2 $\pm$ 0.5 nm. The root-mean-square roughness of the disk was 0.53 $\pm$ 0.07 nm. Although the roughness was statistically no different from that of sample DI-1, the topographic image shows that the number of droplets was much higher than in sample DI-1. When imaged a year later, the polystyrene film had coalesced and formed droplets with an average diameter of 250–350 nm and an average thickness of 35–45 nm (Fig. 9).

Samples with different initial styrene concentrations (series DII)

Sample DII-1 had a ratio of adsorbed C_{16}TAB to adsolubilized monomer of 2:1. We observed several polystyrene droplets and holes on top of a smooth surface (polymer or silica). In Figure 10, droplets of various sizes can be seen in both the topographic and phase images. Although there is no significant differ-

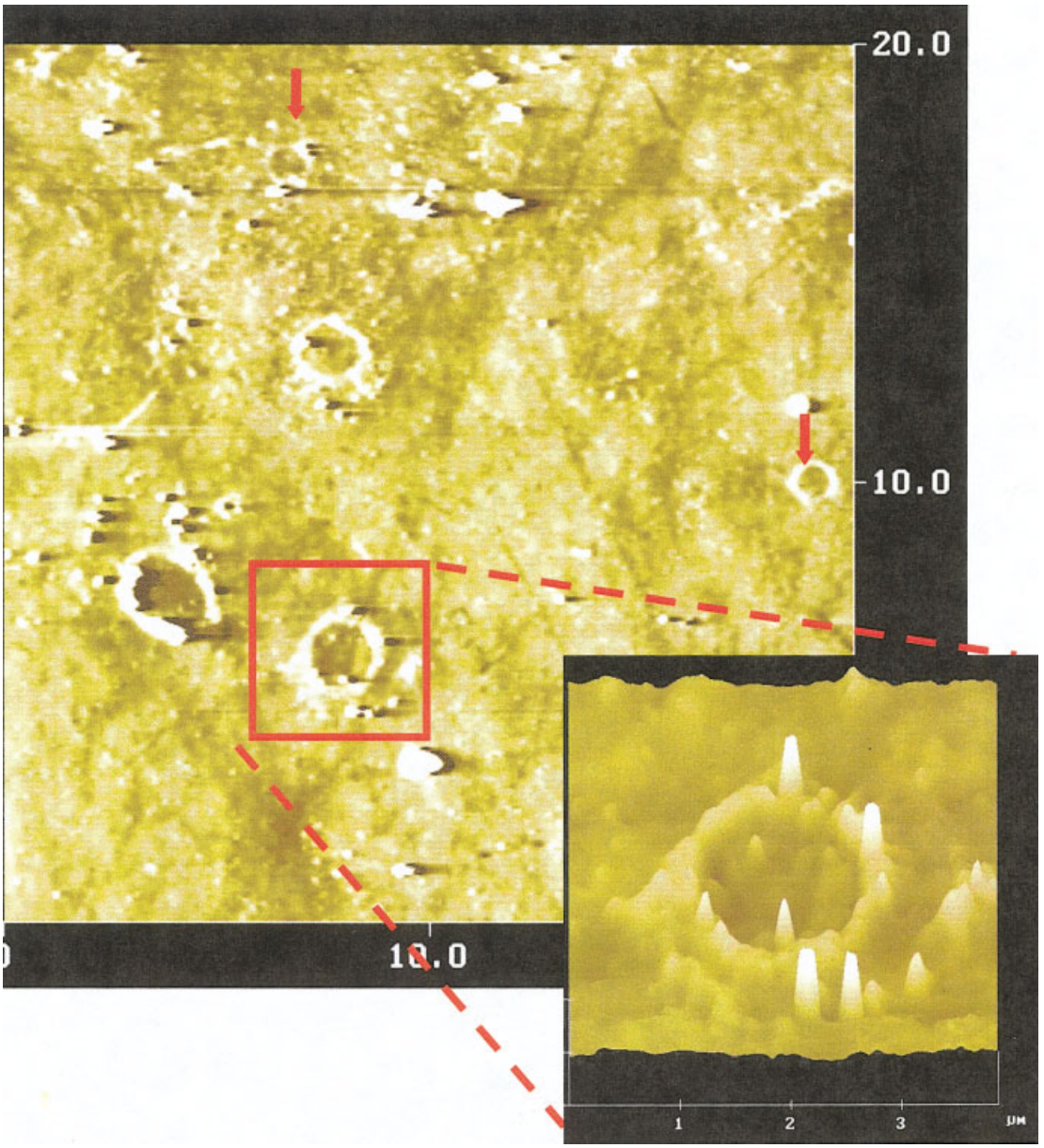

Figure 4 Microscopic topographic image of sample DI-1 (modified by a feed of 750 μM C_{16}TAB and 893 μM styrene) scanned after a year. A ringlike formation of aggregates can be observed, with the larger rings having diameters greater than 1 μm and the smaller rings having diameters of 300–750 nm. The imaging area is 20 μm $\times$ 20 μm, with a z range of 15 nm. The enclosed area shows a three-dimensional image of a ring at 4 μ $\times$ 4 μm, with a z range of 15 nm.

ence in the phase contrast, the edges of these aggregates can clearly be observed. The root-mean-square roughness of the smooth areas was 0.23 nm, giving evidence that the surface was coated by a layer of a polystyrene film. The polystyrene droplets had dimensions of approximately 50 nm $\times$ 98 nm, with heights of approximately 2.8 nm. At a moderate tapping force, some of these droplets were deformed by the tip (Fig. 11).

When the amount of the adsolubilized monomer was decreased to a ratio of the adsorbed surfactant to the adsolubilized monomer of 2.5: 1 (sample DII-2), the formed polymer surface was easily deformed by an external force. At a light tapping force (set-point ratio of 0.9), a rather smooth surface with a root-mean-square roughness of 0.38 $\pm$ 0.07 nm was observed. The phase images show no significant differences in the phase shift, indicating a homogenous polystyrene film present on the silica surface [Fig. 12(a)]. However, under a moderate tapping force (set-point ratio of 0.5), the polystyrene film was deformed or removed, exposing the silica surface beneath. At this applied force, the darker contrast in the phase mode indicated the presence of a soft polystyrene film on top of a hard silica surface [Fig. 12(b)]. The root-mean-square roughness increased to 0.44 $\pm$ 0.05 nm. The average

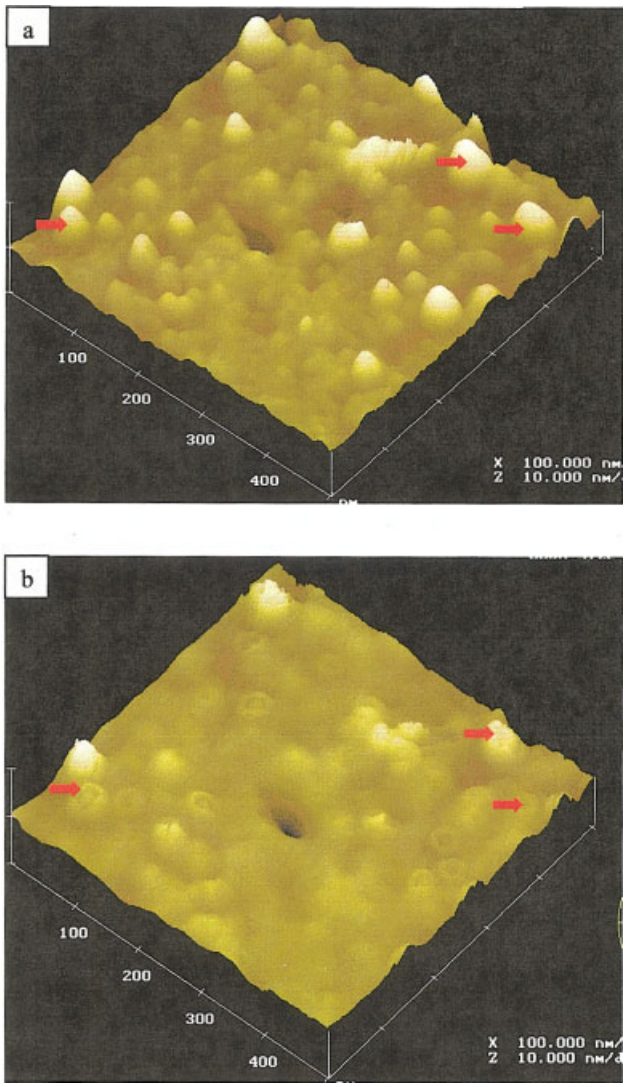

Figure 5 Topographic images of sample DI-2 (500 μM C_{16}TAB and 595 μM styrene) with the imaging performed at the same location under (a) light and (b) high forces. The imaging area is 400 nm × 400 nm, with a z range of 10 nm. The arrows indicate the collapse of the droplets, exposing the interior material.

thickness of the polystyrene film was 0.83 ± 0.12 nm. Some of the deformation of the polystyrene film was reversible, with images returning to their original shape when imaged again under a light tapping force. The time for the film to recover was approximately 45 min. (The surface covered with polystyrene film was imaged under a higher force, with a set-point ratio of less than 0.5, and deformation of the film was observed. A lower scanning force, with a set-point ratio of approximately 1.0, was applied later at a constant y movement of the tip. The time for the recovery of the polystyrene film was recorded. The deformed polystyrene film was said to be recovered when the contrast observed in the topography and phase images no longer changed.)

Polystyrene droplets were observed on the surface of the modified silica when the ratio of adsorbed C_{16}TAB to the adsolubilized monomer was decreased to 3.33:1. Topographic images of sample DII-3 (Fig. 13) are almost identical to those of sample DI-3 (Fig. 5). The average diameter of the droplets was also close to those found in sample DI-3 (37.89 ± 6.9 nm). The average height of these polystyrene droplets was 2.26 ± 0.7 nm, significantly less than that of sample DI-3. The root-mean-square roughness was 0.7 ± 0.22 nm. These droplets were located on top of a thin polymer layer that could be removed by tip imaging under a higher tapping force. Figure 13 shows where a portion of the polystyrene film and droplets were removed, exposing the silica surface beneath. The exposed silica surface can be differentiated from the polystyrene film with the three-dimensional topographic images. The thickness of the polystyrene film was 1.4 nm.

When the ratio of adsorbed C_{16}TAB to the adsolubilized monomer was reduced to 10:1 (sample DII-4), the polystyrene film agglomerated and formed large and irregular structures (Fig. 14). The root-mean-square roughness of the sample was 1.27 ± 0.26 nm.

DISCUSSION

Samples with a constant surfactant/monomer ratio and different feed concentrations

The morphology of the polystyrene film was different for different loadings of C_{16}TAB and styrene. At C_{16}TAB equilibrium concentrations near the critical micelle concentration, the adsorbed surfactant molecules should completely cover the surface of the silica disk. Under this condition, the relatively homogenous surface should allow the styrene monomer to adsolubilize evenly. Therefore, upon polymerization, a thin film of polystyrene should form on the surface when sufficient styrene monomer is present. A uniform film was observed, however, only when the monomer loading was high, as in samples DI-1 and DII-1. In samples DI-1 and DII-1, droplets were observed on top of the smooth film, with more droplets seen for DI-1. These droplets on top of the smooth film may be due to the polymerization of the phase-separated styrene monomer inside the admicelle, which was then deposited on the more uniform film beneath.[15] In sample DI-1, for which the styrene monomer feed was 40,000 times greater than that of the adsorbed surfactant, it was possible that even in the absence of micelles, some of the monomer might have polymerized in the bulk, although there has been little evidence of this in past work. The polymer that polymerized in the bulk supernatant could adsorb on the surface during the washing and drying process, forming globules.[1] Therefore, the surface of sample DI-1 appeared to be more complex than the surface of sample DII-1 and

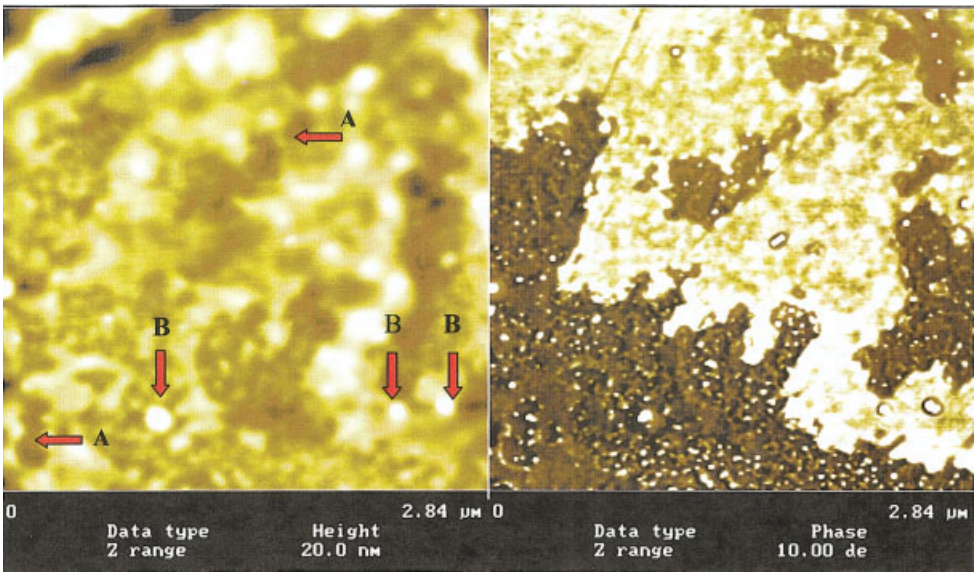

Figure 6 Microscopic topographic image of sample DI-2 (500 μM C_{16}TAB and 595 μM styrene) scanned after a year (left). The uniform polystyrene film coexists with patches of disturbed and irregular structures. Some of the film appears to be folding (arrow A), and some appears to be nucleated (arrow B). The imaging area is 2.84 μm $\times$ 2.84 μm, with a z range of 20 nm and a phase contrast of 10°.

had a higher root-mean-square roughness, as examined under AFM. In sample DII-1, the feed concentration of the styrene monomer was equal to 50% of the adsorbed surfactant. Therefore, if we consider a bilayer in which every two surfactant molecules adsolubilize one monomer molecule, we would expect a thin film approximately one molecule thick to form on the surface during polymerization. In our case, however, we observed a uniform thin film with droplets of polystyrene on the surface in sample DII-1 (Fig. 10). This film was clearly multilayered. A possible explanation for this is that adsolubilization is not uniform throughout the admicelle, as the admicelle may not be uniform because of the presence of higher and lower energy areas. A second explanation of nonhomogeneous adsolubilization could be that, even if the surface is evenly covered by adsorbed surfactant at equilibrium, the adsolubilized monomer will be unevenly

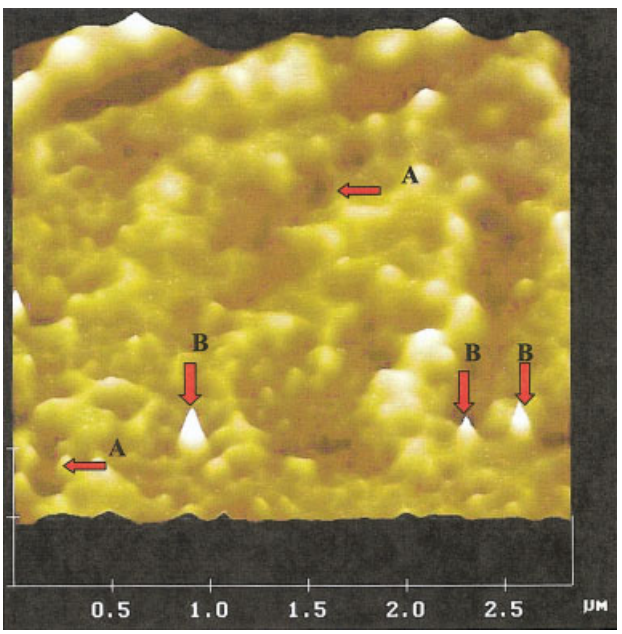

Figure 7 Three-dimensional topographic image of sample DI-2 (500 μM C_{16}TAB and 595 μM styrene) scanned after a year. The uniform polystyrene film coexists with patches of disturbed and irregular structures. Some of the film appears to be folding (arrow A), and some appears to be nucleated (arrow B). The imaging area is 2.84 μm $\times$ 2.84 μm, with a z range of 20 nm.

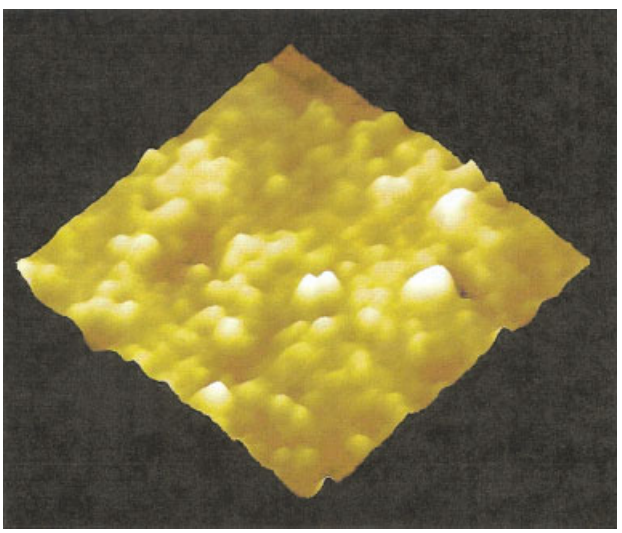

Figure 8 Topographic image of sample DI-4 (50 μM C_{16}TAB and 58 μM styrene). The imaging area is 400 nm $\times$ 400 nm, with a z range of 10 nm.

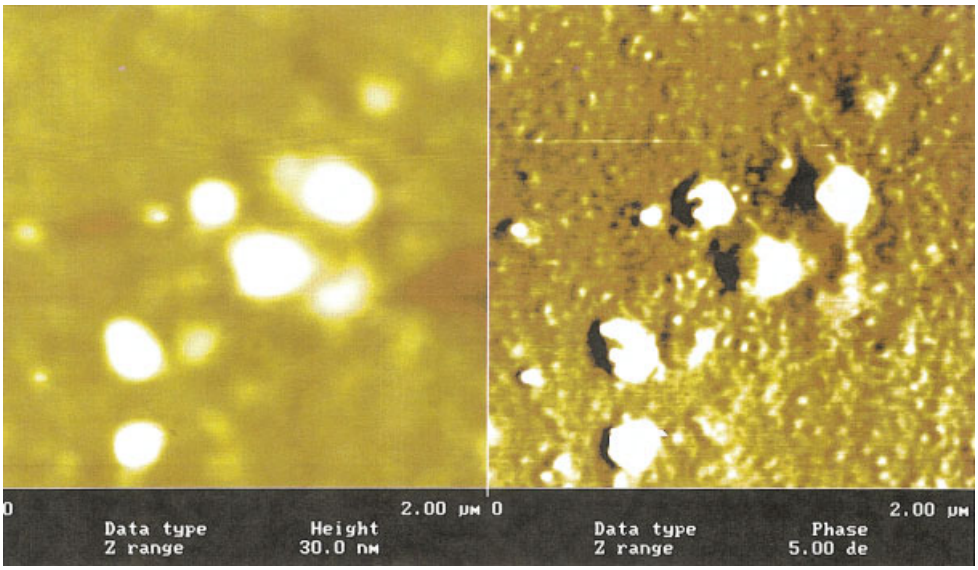

Figure 9 Microscopic topographic images of sample DI-4 after a year. The imaging area is 400 nm × 400 nm, with a *z* range of 10 nm and a phase contrast of 5°. The polystyrene film coalesces and forms patches of aggregates on top of the silica disk.

distributed because of the influence of the long-range van der Waals force between the silica substrate and the adsolubilized monomer. The influence of long-range van der Waals forces (over several hundreds of nanometers) on polymeric solutions on nonwettable surfaces has been observed.[16,17] The monomer that adsolubilized inside the admicelle could, therefore, tend to coalesce and form droplets or patches more than one molecule thick. Some holes would be expected to occur because of a material shortage in some regions. A third possibility is that even if the adsolubilization is homogeneous, there is agglomeration during the dewetting/drying process. More *in situ* work will be needed to determine the actual mechanisms involved.

After the samples were kept for a year inside a dry environment (relative humidity < 12%), the polystyrene film was no longer uniformly adsorbed on the silica surface but had migrated, forming larger aggregates. The reason for the ring and straight-line structures that were observed is still under investigation. One possibility is that they may due to different film–surface interaction forces on a heterogeneous surface, which comes into play after the removal of the surfactant.[18]

The droplets observed in sample DI-2 (Fig. 5) can be explained as follows. If a uniform polymer layer forms during polymerization, this thin film is exposed first to water and then to air during the surfactant removal step. The thin film should experience instability if exposed to long-range repulsive van der Waals forces.[19] The value of the long-range term in the van der

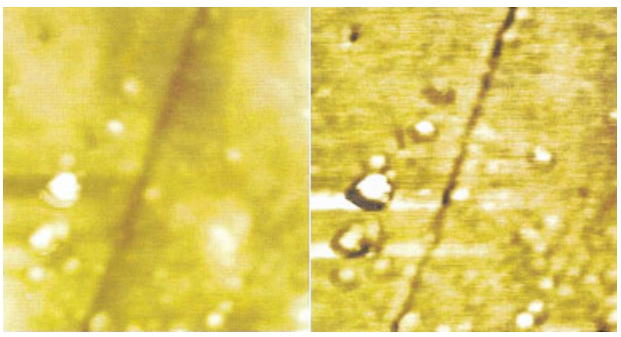

Figure 10 Topographic image (left) and phase image (right) of sample DII-1 (2:1 ratio of adsorbed C_{16}TAB to adsolubilized styrene). The imaging area is 500 nm × 500 nm, with a *z* range of 5 nm and a phase contrast of 30°.

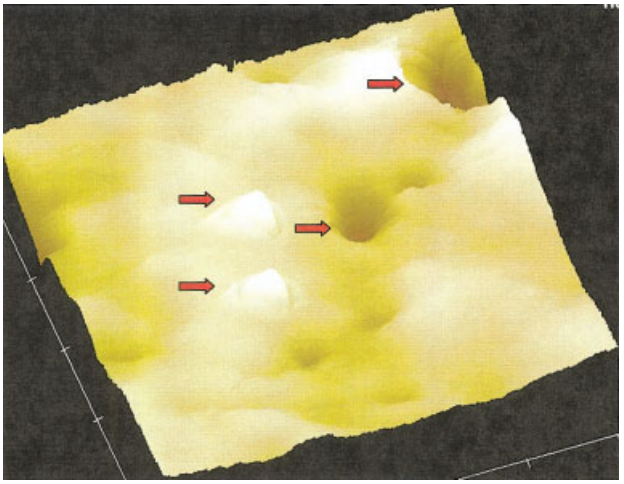

Figure 11 Three-dimensional topographic image of sample DII-1 (maximum surfactant adsorption and 2:1 ratio of adsorbed C_{16}TAB to adsolubilized styrene). The imaging area is 500 nm × 500 nm, with a *z* range of 5 nm. The arrows indicate deformed polystyrene droplets and holes.

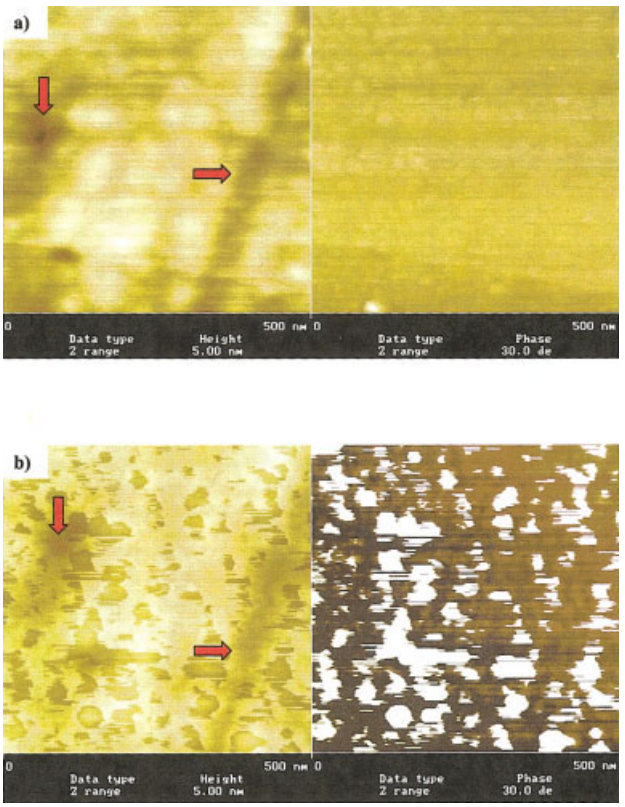

Figure 12 Topographic images of sample DII-2 (2:0.8 ratio of adsorbed C_{16}TAB to adsolubilized styrene) imaged with setpoint ratios of (a) 0.9 and (b) 0.5. The imaging area is 500 nm × 500 nm, with a z range of 5 nm and a phase contrast of 30°.

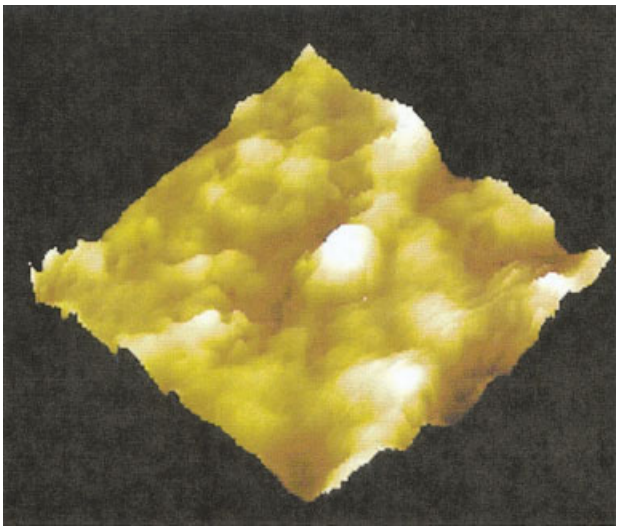

Figure 14 Three-dimensional topographic image of sample DII-4 (2:0.2 ratio of adsorbed C_{16}TAB to adsolubilized styrene). The imaging area is 500 nm × 500 nm, with a z range of 5 nm. The surface is covered by a polystyrene network.

Waals force can be determined by the effective Hamaker constant A_{eff}: $F(h) = A_{\text{eff}}/12\pi h^2$. For a thin film on top of a homogeneous solid substrate immersed in a medium, A_{eff} is the difference between A_{sf}, the Hamaker constant between the solid and the film, and A_{ff}, the Hamaker constant of the film: $A_{\text{eff}} = A_{ff} - A_{sf}$. If A_{eff} is less than 0, the film is said to be unstable. With Hamaker constants of 7.95×10^{-20} J for A_{si-si} (the interaction between silica and silica)[20] and 6.6×10^{-20} J for A_{ps-ps} (the interaction between polystyrene and polystyrene),[21] we obtain an A_{eff} value that is always less than zero. This says that the observed film should be unstable and have a tendency to thin. However, we observed droplets deposited on a uniform polystyrene

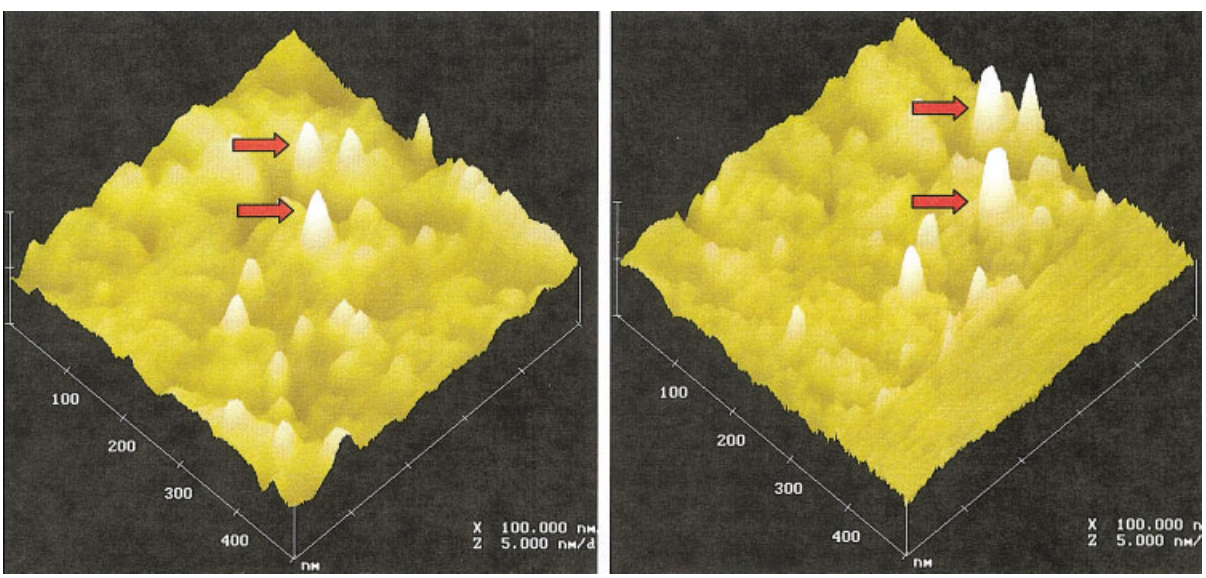

Figure 13 Three-dimensional topographic images of sample DII-3 (2:0.6 ratio of adsorbed C_{16}TAB to adsolubilized styrene). The imaging area is 500 nm × 500 nm, with a z range of 5 nm. The arrows show nucleated polystyrene. The polystyrene film is deformed by the tip after imaging at a higher tapping force. The average thickness measured across the deformed and undeformed polystyrene film is 1.4 nm.

film on the surface in sample DI-2. This may be due to the presence of a whole or partial monolayer of C_{16}TAB under the polymer adsorbed on the surface of the silica. If this surfactant layer exists, then the effective Hamaker constant between the polystyrene film and the silica surface, now separated by a monolayer of C_{16}TAB, is given by[22]

$$A_{eff} \approx A_{mf} - A_{ff} + \frac{A_{sf} - A_{mf}}{(1 + X)^3}$$

where A_{mf} is the Hamaker constant between the monolayer of C_{16}TAB and polystyrene. X is the ratio of the thickness of the adsorbed surfactant to the thickness of the polymer film. This equation, however, neglects the influence of the electrostatic interaction force. If we assume that sufficient surfactant remains to neutralize the surface charge, we only need to calculate the interaction force between the silica and the polymer–air interface. With this approach, the critical thickness of the polymer layer needed to form a stable film (in the presence of a C_{16}TAB monolayer) has to be greater than 4 nm. Below this critical thickness, the film will be unstable, and surface undulations or spinodal decomposition will be observed.[23,24] Therefore, the instability caused by the long-range van der Waals forces will eventually rupture the film, causing the formation of patches or polymer droplets.[23,24]

When the samples were reimaged after almost a year to test this prediction, a uniform layer of a polystyrene film coexisting with some bicontinuous patches was observed in sample DI-2 (Fig. 6). We can conclude that a layer of the adsorbed surfactant at the polystyrene–silica interface likely existed and that the thickness of the polymer film in sample DI-2 was between 5 and 10 nm, which agrees well with our prediction.

When the concentration of C_{16}TAB was reduced to only 6.5% of the maximum adsorption, only patchy admicelles should have existed on the silica surface. In sample DI-4, the concentration of the styrene monomer was still very high. Therefore, we postulate that some of the polymerization reaction might have occurred in the bulk and that the polymer aggregates so formed adhered to the silica during the washing and drying steps. A second possibility is that the monomer diffusing into the patches during polymerization formed large aggregates during the polymerization process. The dimensions of the droplets were close to those observed in sample DI-1. When we scanned the sample a year later, the film was shown to be unstable and to have formed larger aggregates, with diameters of 250–350 nm and heights of 35–45 nm, scattered across the surface of the disk (Fig. 9).

Samples with constant C_{16}TAB and different monomer concentrations

In this series, we found that the formed polymer film was stable over time, remaining as an extended layer on the silica disk. The presence of the adsorbed surfactant on the surface kept the thin film stable at a styrene monomer concentration of up to 8.67 n*M*. We can see from the topographic images of samples DII-1 and DII-2 (Figs. 10 and 12) that the polystyrene film was quit uniform. However, droplets and holes started to form when the feed styrene concentration was reduced to 6.5 n*M*. Below this concentration, the film experienced instability, and droplets formed (sample DII-3; Fig. 13). The formation of these droplets can possibly be explained by either the dewetting effect due to the long-range van der Waals interaction or the nucleation of polystyrene during polymerization. Because the morphology of sample DII-3 was close to that of DI-2, it is likely that the droplets formed for the same reason as those observed in sample DI-2. However, further investigation is needed to determine the mechanism of droplet formation.

At the lowest feed concentration of the monomer, styrene monomers could either adsolubilize evenly inside the admicelle or pool together within the admicelle. If we believe that they evenly adsolubilized, we should expect the formation of a thin polystyrene film after the polymerization that could easily be deformed by external forces. Therefore, with the removal of C_{16}TAB molecules during washing and drying, the film was redistributed, and this led to the formation of these irregular structures. If the monomers pooled within the admicelle during the adsolubilization or polymerization, we would expect to see the formation of droplets. Therefore, after washing and drying, the droplets would remain as observed.

CONCLUSIONS

Tapping-mode AFM was used to examine a polystyrene-modified silica disk formed by the admicellar polymerization process. Modified with a constant feed ratio of C_{16}TAB to styrene of 1:1.2, polystyrene droplets were observed at all concentrations, from sample DI-1 (750 μM C_{16}TAB and 863 μM styrene) to sample DI-4 (50 μM C_{16}TAB and 58 μM styrene), with larger droplets observed at medium loadings. When samples were examined again after 1 year, the polystyrene films had agglomerated, forming larger aggregates arranged in straight-line or ringlike structures at higher feed concentrations. At medium feed levels, bicontinuous films were observed. At low loadings, larger polystyrene aggregates scattered on the silica surface were observed.

Silica disks modified with constant C_{16}TAB concentrations (at the maximum adsorption) and various

styrene loadings were also studied. The polymer tended to form uniform films at high styrene concentrations. At styrene feed concentrations below 6.5 n*M*, the formed films became unstable, with droplets and holes forming.

Unlike our previous work on amorphous silica,[25] the morphology of a polymer formed on a flat silica surface is affected by the amounts of the adsorbed surfactants. When the coverage of the adsorbed surfactant is low, the polymer film will be less stable, and aggregations will occur immediately. At maximum coverage, a uniform thin film will form when there is enough styrene monomer. The stability of the polymer film is thought to be caused by the presence of a monolayer of C_{16}TAB at the polystyrene–silica interface. The morphology of the polymer formed may be the result of uneven adsolubilization of the monomer(s) or the interaction between the silica substrate and polymer surface during the dewetting mechanism.

References

1. Sakhalkar, S. S.; Hirt, D. E. Langmuir 1995, 11, 3369.
2. Wu, J. Y.; Harwell, J. H.; O'Rear, E. A. J Phys Chem 1987, 91, 623.
3. Wu, J. Y.; Harwell, J. H.; O'Rear, E. A. AIChE J 1988, 34, 1511.
4. Lai, C. L.; Harwell, J. H.; O'Rear, E. A. Langmuir 1995, 11, 905.
5. Waddell, W. H.; O'Haver, J. H.; Evans, L. R.; Harwell, J. H. J Appl Polym Sci 1995, 55, 1627.
6. Thammathdanukul, V.; O'Haver, J. H.; Harwell, J. H.; Osuwan, S.; Na-Ranong, N.; Waddell, W. H. J Appl Polym Sci 1996, 59, 1741.
7. O'Haver, J. H.; Harwell, J. H.; Evans, L. R.; Waddell, W. H. J Appl Polym Sci 1996, 59, 1427.
8. O'Haver, J. H.; Harwell, J. H.; O'Rear, E. A.; Snodgrass, L. J.; Waddell, W. H. Langmuir 1994, 10, 2588.
9. Chen, H.-Y. Master Thesis, University of Oklahoma, 1992.
10. Grady, B. P.; O'Rear, E. A.; Penn, L. S.; Pedicini, A. Polym Compos 1998, 19, 579.
11. Genetti, W. B.; Yuan, W. L.; Grady, B. P.; O'Rear, E. A.; Lai, C. L; Glatzhofer, D. T. J Mater Sci 1998, 33, 3085.
12. Dickson, J. Master Thesis, University of Mississippi, 2001.
13. Rosen, M. J. Surfactants and Interfacial Phenomena, 2nd ed.; Wiley: New York, 1989.
14. Iler, R. K. The Chemistry of Silica: Solubility, Polymerization, Colloid and Surface Properties, and Biochemistry; Wiley: New York, 1979.
15. Wu, J. Ph.D. Dissertation, University of Oklahoma, 1987.
16. Brochard-Wyart, F.; Daillant, J. Can J Phys 1990, 68, 1084.
17. Reiter, G. Langmuir 1993, 9, 1344.
18. Kargupta, K.; Konnur, R.; Sharma, A. Langmuir 2000, 16, 10243.
19. Xie, R.; Karim, A.; Douglas, J. F.; Han, C. C.; Weiss, R. A. Phys Rev Lett 1998, 81, 1251.
20. Bergstrom, L. Adv Colloid Interface Sci 1997, 70, 125.
21. Israelachvilli, J. N. Intermolecular and Surface Forces; Academic: London, 1985.
22. Kerle, T.; Yerushlami-Rozen, R.; Klein, R.; Fetters, R. Europhys Lett 1998, 44, 484.
23. Segalman, R. A.; Green, P. F. Macromolecules 1999, 32, 801.
24. Xie, R.; Karim, A.; Douglas, J. F.; Han, C. C.; Weiss, R. A. Phys Rev Lett 1998, 81, 1251.
25. Chun, H. S.; O'Haver, J. H. J Appl Polym Sci 2003, 87, 290.